2017 21st International Conference on Process Control (PC)
June 6–9, 2017, Štrbské Pleso, Slovakia

Finite Element Method Based Modeling of a Flexible Wing Structure

Filip Svoboda
Czech Technical University in Praque,
Faculty of Electrical Engineering
Karlovo náměstí 13/E,
12135 Prague, Czech Republic
Email: svobofi2@fel.cvut.cz

Martin Hromčík
Czech Technical University in Praque,
Faculty of Electrical Engineering
Karlovo náměstí 13/E,
12135 Prague, Czech Republic
Email: xhromcik@fel.cvut.cz

***Abstract*—The finite element based structural model of a flexible wing is presented. The structural model will be a part of a servoelastic wing used for flutter analysis and designing flutter suppression control systems. It also allows modal analysis of a wing with given parameters. A finite element model consists of Euler-Bernoulli beams joined together. This approach is able to reach high accuracy and various properties of a particular wing element can be modeled.**

1. Introduction

As part of an active flutter suppression research project, we develop a structural model for dynamics analysis and control designs for a flexible wing. Aeroelastic flutter [15] is a phenomenon which causes dynamic instability of a flexible structure like a wing in airflow. Unstable oscillations occur with an interaction of aerodynamics and structural dynamics. The range of an aircraft operating conditions is determined to prevent flutter. The first way to expand the flutter boundary is a change in a mechanical design of an aircraft which can lead to additional mass and deterioration of efficiency. Active flutter suppression is a solution to ensure sufficient operating range of an aircraft in a more efficient manner.

This paper focuses on the structural model of a servoelastic wing model depicted in Figure 1. It consists of structural dynamics, aerodynamics and dynamics of an actuator (flap). Dynamics interconnection is introduced in [11] or [8]. Aerodynamic block calculating lift distribution on the oscillating surface usually uses Doublet Lattice Method (DLM) in the subsonic flow described by Rodden in [10]. The above mentioned methods are also used in the NASTRAN software documented in [7].

The assembled model shall be used in the future for designing active flutter dampers. Many principles have been presented in the literature. For example pole/zero loci design [16], linear quadratic Gaussian control, nonlinear control [17], adaptive control [18], linear parameter-varying control [19], [20], or H_∞ synthesis. One of the applications of a robust control for small flexible aircraft is reported in [13].

The finite element method approach (FEM), which will be used extensively in this paper, is a numerical technique

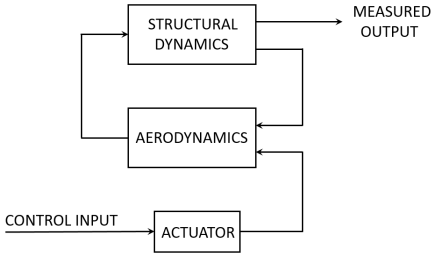

Figure 1. Aeroservoelastic wing schema.

for finding approximate solutions of problems discribed by partial differential equations [1], [3], or [12]. One of the examples can be a flexible structure. The structure is spatially descretized into finite elements; in this way the PDE formulation is transformed into large sets of ODEs. High fidelity of FEM models for flutter control applications can be achieved as shown in [2] where the simulations and measured flight data are compared. Note also that model parameters can be obtained from ground vibration tests [9] and [6].

The paper is organized as follows. The principles of FEM and their application in a wing flexible structure is introduced in Section 2. It also deals with State–Space representation suitable for further analysis and modeling. Section 3 focuses on modal analysis. Natural frequencies and mode shapes are calculated and visualized. Time domain simulations are shown in Section 4. Finally, the concluding remarks and further research proposals are presented in Section 5.

The presented manuscript presents the part of authors ongoing research on active flutter suppression solutions for small sports aircraft. Related previous achieved results are summarized in the recent MSc. diploma thesis [14] focusing on 2D aeroelastic airfoil model and its analysis, controller design and experiments in wind tunnel. A paper on fixed–order H_∞ control for the same setup design has been submitted recently to IFAC 2017 World Congress [21].

978-1-5386-4011-1/17/$31.00

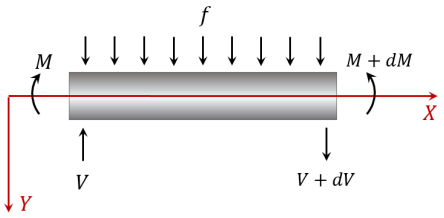

Figure 2. Euler–Bernoulli beam.

2. FEM based model

The goal of this section is to describe principles of a FEM modeling of a flexible wing. The structural model is based on Euler–Bernoulli beam theory which considers small displacements and linear elastic material, therefore, the Hooks law is valid. The beam with applied forces V and torques M is in Figure 2. Resulting equations (1), (2), (3), (4), are summarized below.

$$(V + dV) - V + f dx = 0 \tag{1}$$

$$(M + dM) - M - V dx + f dx \frac{dx}{2} = 0 \tag{2}$$

$$\frac{dV}{dx} = -f \tag{3}$$

$$\frac{dM}{dx} = V \tag{4}$$

For deriving equations of motion, the kinematics must be determined. Equations (5), (6) are considered for small displacements, where θ is the radius of the deflection curve, u is transverse displacement, E is Youngs modulus of elasticity and I is the moment of area.

$$\theta = -\frac{du}{dx} \tag{5}$$

$$M = EI\frac{d\theta}{dx} \tag{6}$$

By substitutions in equations (3), (4), (5) and (6) equations (7) and (8) can be written. The Euler–Bernoulli beam equation (9) is derived from them.

$$\frac{d^2M}{dx^2} = -f \tag{7}$$

$$EI\frac{d^2u}{dx^2} = -M \tag{8}$$

$$EI\frac{d^4u}{dx^4} = -f \tag{9}$$

For solving Euler–Bernoulli beam equation, the boundary conditions (10) must be added. Solution can be found by Galerkins method. It means every function can be written as a linear combination of basis functions. Rather then basis

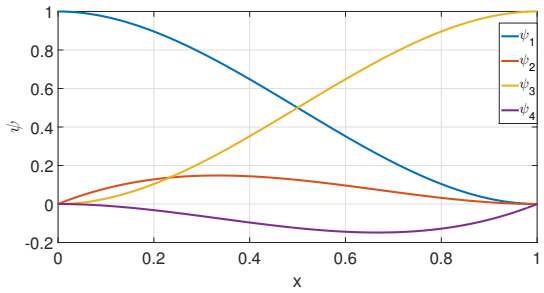

Figure 3. Shape functions for a beam element.

functions, the shape functions $\psi_j(x)$ are used. Solution is described in approximation (11), where $\alpha = \begin{bmatrix} v_{i-1} \\ \theta_{i-1} \\ v_i \\ \theta_i \end{bmatrix}$. Shape functions $\psi = \begin{bmatrix} \psi_1 & \psi_2 & \psi_3 & \psi_4 \end{bmatrix}$ are cubic Hermite polynomials (Lovest order polynomials that satisfy continuity requirements). Shapes of functions (12) are shown in Figure 3.

$$\begin{aligned} u(x=0) &= v_1 \\ u(x=L) &= v_2 \\ \frac{du}{dx}|_{x=0} &= \theta_1 \\ \frac{du}{dx}|_{x=L} &= \theta_2 \end{aligned} \tag{10}$$

$$u_h(x) = \sum_{j=1}^{4} \alpha_j \psi_j(x) \tag{11}$$

$$\begin{aligned} \psi_1(x) &= \frac{1}{L^3}(2x^3 - 3x^2L + L^3) \\ \psi_2(x) &= \frac{1}{L^3}(x^3L - 2x^2L^2 + xL^3) \\ \psi_3(x) &= \frac{1}{L^3}(-2x^3 + 3x^2L) \\ \psi_4(x) &= \frac{1}{L^3}(x^3L - x^2L^2) \end{aligned} \tag{12}$$

After substitution to equation 9 and integration (13), the equation can be rewritten to (14), where k_e is the element stiffness matrix and f_e is a load. Similarly, element mass matrix m_e can be derived.

$$\left(\int_{x_{i-1}}^{x_i} EIB^TB\right)\alpha dx = \int_{x_{i-1}}^{x_i} fN^T dx \tag{13}$$

$$k_e\alpha = f_e \tag{14}$$

For our flexible wing structural model, the torsional degree of freedom is added to Euler–Bernoulli beam. The beam element with nodes $i-1$ and i with three degrees of freedom (DoF) is shown in Figure 4. Appropriate element

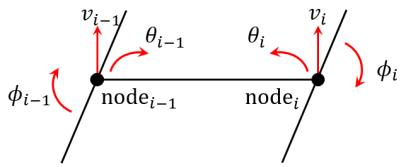

Figure 4. The beam element with three degrees of freedom.

mass and stiffness matrix are presented in (15) and (16), where m_l is mass per unit length, j_l is inertia per unit length, G is modulus of rigidity, I_z is moment of area and L is a length of a beam. Columns in the matrixes corresponds to vector $x_e = \begin{bmatrix} v_{i-1} & \theta_{i-1} & \phi_{i-1} & v_i & \theta_i & \phi_i \end{bmatrix}^T$.

$$k_e = \begin{bmatrix} \frac{12EI_z}{L^3} & \frac{6EI_z}{L^3} & 0 & \frac{-12EI_z}{L^3} & \frac{6EI_z}{L^2} & 0 \\ \frac{6EI_z}{L^2} & \frac{4EI_z}{L} & 0 & \frac{-6EI_z}{L^2} & \frac{2EI_z}{L} & 0 \\ 0 & 0 & \frac{GJ_x}{L} & 0 & 0 & \frac{-GJ_x}{L} \\ \frac{-12EI_z}{L^3} & \frac{-6EI_z}{L^3} & 0 & \frac{12EI_z}{L^3} & \frac{-6EI_z}{L^2} & 0 \\ \frac{6EI_z}{L^2} & \frac{2EI_z}{L} & 0 & \frac{-6EI_z}{L^2} & \frac{4EI_z}{L} & 0 \\ 0 & 0 & \frac{-GJ_x}{L} & 0 & 0 & \frac{GJ_x}{L} \end{bmatrix} \tag{15}$$

$$m_e = \begin{bmatrix} \frac{156m_lL}{420} & \frac{22m_lL^2}{420} & 0 & \frac{54m_lL}{420} & \frac{-13m_lL^2}{420} & 0 \\ \frac{22m_lL^2}{420} & \frac{4m_lL^3}{420} & 0 & \frac{13m_lL^2}{420} & \frac{3m_lL^3}{420} & 0 \\ 0 & 0 & \frac{j_lL}{3} & 0 & 0 & \frac{j_lL}{6} \\ \frac{54m_lL}{420} & \frac{13m_lL^2}{420} & 0 & \frac{156m_lL}{420} & \frac{-22m_lL^2}{420} & 0 \\ \frac{-13m_lL^2}{420} & \frac{-3m_lL^3}{420} & 0 & \frac{-22m_lL^2}{420} & \frac{4m_lL^3}{420} & 0 \\ 0 & 0 & \frac{j_lL}{6} & 0 & 0 & \frac{j_lL}{3} \end{bmatrix} \tag{16}$$

The beam element represents the element of a wing. Different properties in each wing section can be modeled by different properties of a beam. Finally, the whole wing is a connection of that beams. The acquired system is described by equation (17). The matrix M_w and K_w are wing mass and stiffness matrices composed from element matrices. Their size is $[3n \times 3n]$, the number of DoF times number of nodes respectively. Figure 5 shows the principle of M_w and K_w calculation. Vector $X = \begin{bmatrix} v_1 & \theta_1 & \phi_1 & v_2 & \theta_2 & \phi_2 & \dots & v_n & \theta_n\phi_n \end{bmatrix}^T$ contains displacement variables of each node. Nodes forces and torques represents vector F_w.

$$M_w\ddot{X} + C_w\dot{X} + K_wX = F_w \tag{17}$$

This structural wing model consider one end clamped wing that means a rigid connection between the first node and stationary fuselage. The connection is simulated by setting high coefficients the mass and stiffness matrix in positions corresponding to node 1 (v_1, θ_1, ϕ_1).

Damping matrix C_w from equation (17) can be obtained in different ways. Rayleigh damping can be considered for example. It assumes that the damping matrix is a linear combination of the mass and stiffness matrices $C_w = a_0M_w + a_1K_w$.

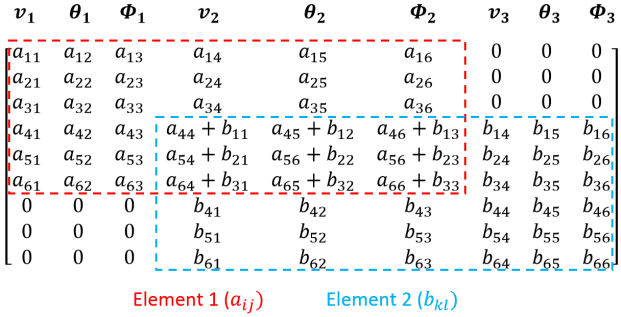

Figure 5. Principle of M_w and K_w structure for two elements.

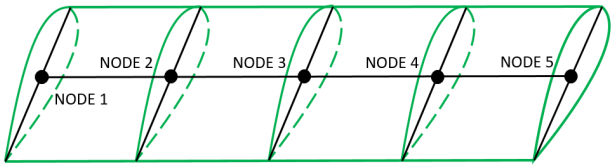

Figure 6. Wing elements.

2.1. State–Space model

Structural dynamics is just one part of an aeroservoelastic model (Figure 1) containing aerodynamics and dynamics of an actuator. For further work with the model, it is useful to transform equation (17) to state–spece model. Forces and torques will be as inputs to the system(F_w) and the accelerations $\ddot{X}$ will be an output. After substitution $X_1 = X$, $X_2 = \dot{X}$, it is possible to rewrite equation (17) to state–space representation (18).

$$\begin{aligned} \dot{X}_1 &= X_2 \\ \dot{X}_2 &= -M_w^{-1}K_wX_1 - M_w^{-1}C_wX_2 + M_w^{-1}F_w \\ y &= -M_w^{-1}K_wX_1 - M_w^{-1}C_wX_2 + M_w^{-1}F_w \end{aligned} \tag{18}$$

TABLE 1. FE WING PARAMETERS

Symbol	Description	Value	Units
L_e	length of the element	0.356	m
w_e	width of the element	0.26	m
h_e	height of the element	0.0065	m
m_{pl}	mass per unit length	0.94	kg/m
j_{pl}	inertia per unit length	0.005	kgm
E	Young's modulus	$2.34 \cdot 10^{10}$	Pa
G	modulus of rigidity	$4.05 \cdot 10^6$	Pa
a_1	mass damping coefficient	0.0001	–
a_2	stiffness damping coefficient	0.0001	–

3. Modal analysis

Modal analysis is closely related to flexible structure modeling. Parameters are usually obtained from static and dynamic tests. Dynamic measurements can be available

in the form of ground vibration tests. This tests, which are required by flutter specifications, measures modes and frequencies of an aircraft. An example of a ground vibration test can be found in [4] and [5].

The model described in equation (17) contains modal damping matrix C_w making dynamics more realistic. However modal analysis can be done with method considering undamped and unforced system (19). Next, assume that this dynamic system makes harmonic motion of circular frequency ω. It can be done using function (20) and corresponding acceleration (21). Then equation (22) can be stated. Term $(K_w - \omega^2 M_w) = D(\omega)$ is called the dynamic stiffness matrix used for solving free vibrations eigenproblem (23). Characteristic equation $q(\omega^2)$ has roots equal to undamped natural circular frequencies. Undamped free–vibrations natural modes are eigenvectors of $D(\omega)$.

$$M_w \ddot{X} + K_w X = 0 \tag{19}$$

$$X(t) = X\cos(\omega t - \varphi) \tag{20}$$

$$\ddot{X}(t) = -\omega^2 X\cos(\omega t - \varphi) \tag{21}$$

$$M_w \ddot{X} + K_w X = (K_w - \omega^2 M_w)X = 0 \tag{22}$$

$$q(\omega^2) = det(D(\omega)) = 0 \tag{23}$$

Finally, if a modal damping ζ is known from ground vibration test, It can be used for derivation of a modal damping matrix C_w as in equation (24).

$$C_w = 2\zeta' diag(\omega) M_w \tag{24}$$

The equation (22) can be rewritten to the canonical form of the generalized algebraic eigenproblem (25), where λ is a diagonal matrix with eigenvalues on the main diagonal and V is a matrix with right eigenvectors. Therefore the square roots of eigenvalues are natural frequencies ω_i and eigenvectors represents the mode shapes.

$$K_w V = M_w V \lambda \tag{25}$$

With considering parameters from table 1, natural frequencies, and modal shapes are computed and stated in table 2 and figures 7, 8, 9 and 10. Same ω_i are apparent from Bode plots in Figure 11.

4. Simulations

This section presents time behavior of a finite element based structural model of a flexible wing. The wing made up five elements with same parameters from Table 1. Chirp signal was used as a source of torque and force in the simulations. Figure 12 is a time response to chirp signal with initial frequency 0 Hz and target frequency 25 Hz. This signal was a source of force to node 5. The peaks

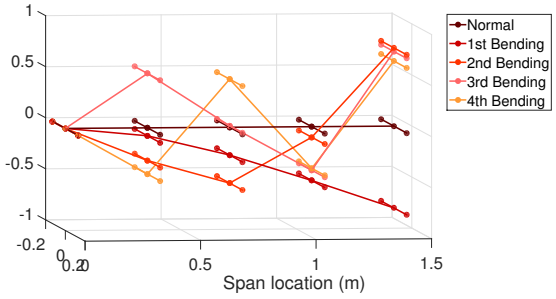

Figure 7. Bending modes shapes.

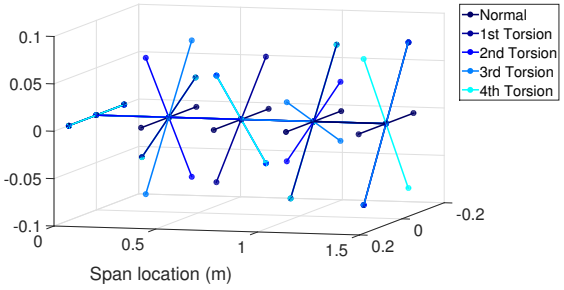

Figure 8. Torsional modes shapes.

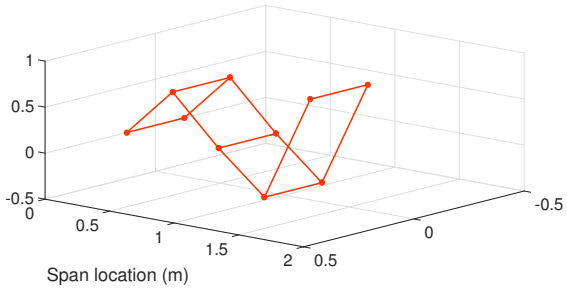

Figure 9. Third bending mode shape.

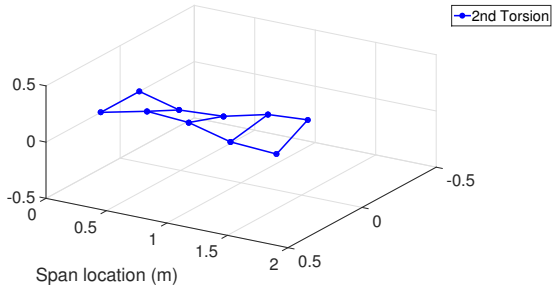

Figure 10. Second torsional mode shape.

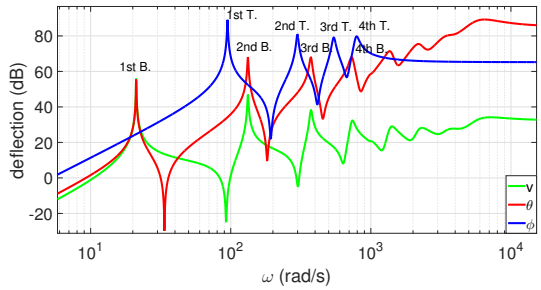

Figure 11. Magnitude Bode plots of transfer functions from force and torques of 5th node to deflections of that node.

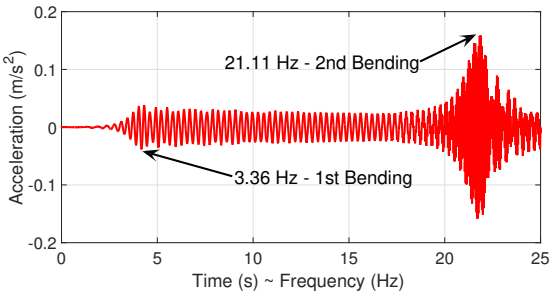

Figure 12. Time response to chirp (0–25 Hz).

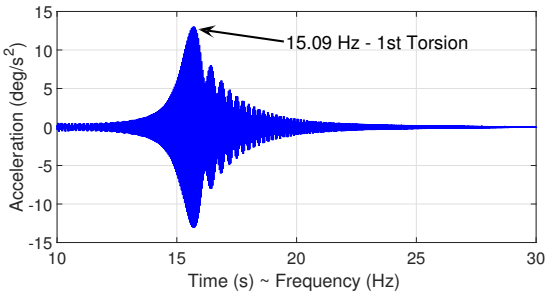

Figure 13. Time response to chirp (10–30 Hz).

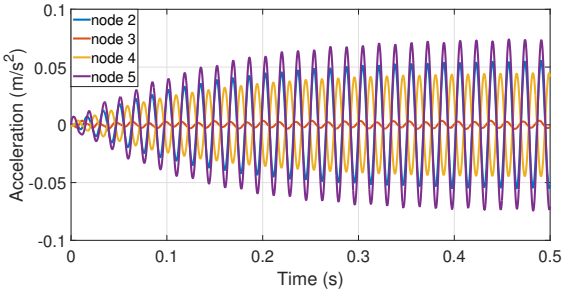

Figure 14. Time response to 59.4 Hz.

in the figure correspond to first and second bending mode. For visualization of a first torsion mode frequency (Figure 13), chirp signal with initial frequency 10 Hz and target frequency 30 Hz was used as a source of torque to node 5. Mode shapes are reflected in phase shifts of each node acceleration. An example is Figure 14, with an acceleration of nodes with third bending mode excitation.

5. Conclusion

The paper describes the principle of a FEM based flexible wing structure modeling. Euler–Bernoulli beam theory was used for wing discretization and equations of motion have been derived. These equations were analyzed and natural frequencies and modal shapes were found. Magnitude Bode plots show natural frequencies as a frequency peaks in a graph. Time simulations also demonstrate system sensitivity to forces and torques at modal frequencies. Flexible wing structure model has a practical use in flutter analysis and synthesis of a flutter suppression systems.

TABLE 2. NATURAL FREQUENCY

ω_i	Description	Value (rad/s)	Frequency (Hz)
ω_1	1st Bending	21.14	3.36
ω_2	1st Torsion	94.82	15.09
ω_3	2st Bending	132.63	21.11
ω_4	2st Torsion	299.12	47.61
ω_5	3st Bending	373.35	59.42
ω_6	3st Torsion	543.37	86.48
ω_7	4st Bending	733.13	116.68
ω_8	4st Torsion	785.76	125.06

Acknowledgment

This research was supported by the Czech Science Foundation (GACR) under contract No. 16-21961S.

References

[1] G.P.Nikishkov, *Introduction to the Finite Element Method*, University of Aizu, Japan: Aizu-Wakamatsu, 2004.

[2] E. L. Burnett and Ch. Atkinson and J. Beranek and B. Sibbitt and B. Holm-Hansen and L. Nicolai, *NDOF Simulation Model for Flight Control Development with Flight Test Correlation*,AIAA Modeling and Simulation Technologies Conference, Ontario Canada: Toronto, August 2010.

[3] S. Dietz and O. Wallrapp and S. Wiedemann, *NODAL VS. MODAL REPRESENTATION IN FLEXIBLE MULTIBODY SYSTEM DYNAMICS*,Multibody Dynamics, Portugal: Lisabon, July 2003.

[4] P. Rossouw, *The flutter analysis of the JS1 glider*, North–West University, Potchefstroom, November 2007.

[5] M. Konvalinka, *FEM Modal and Flutter Analysis of the G304S Glider*, Department of Aerospace Engineering, Faculty of Mechanical Engineering, CTU, Czech Republic: Prague 2010.

[6] W. P. Rodden, *A Method for Deriving Structural Influence Coefficients from Ground Vibration Tests* , AIAA Journal VOL. 5, NO. 5, pp. 991–1000, May 1967.

[7] W. P. Rodden and E. H. Johnson, *MSC/NASTRAN Aeroelastic Analysis: User's Guide, Version 68*, MacNealSchwendler Corporation, 1994.

[8] A. Kotikalpudi and H. Pfifer and G. J. Balas *Unsteady Aerodynamics Modeling for a Flexible Unmanned Air Vehicle*, AIAA Atmospheric Flight Mechanics Conference, AIAA AVIATION Forum, (AIAA 2015-2854).

[9] A.Gupta and C.P. Moreno and H. Pfifer and B. Taylor and G. J. Balas *Updating a finite element based structural model of a small flexible aircraft*, AIAA Modeling and Simulation Technologies Conference, AIAA SciTech Forum, (AIAA 2015-0903).

[10] E. Albano and W. P. Rodden, *A doublet-lattice method for calculating lift distributions on oscillating surfaces in subsonic flows*, AIAA Journal, Vol. 7, No. 2 (1969), pp. 279-285.

[11] B. P. Danowsky and T. Lieu and A. Coderre-Chabot, *Control Oriented Aeroservoelastic Modeling of a Small Flexible Aircraft using Computational Fluid Dynamics and Computational Structural Dynamics - Invited*, AIAA Atmospheric Flight Mechanics Conference, AIAA SciTech Forum, (AIAA 2016-1749).

[12] W. Su and C. E. S. Cesnik *ynamic Response of Highly Flexible Flying Wings*, AIAA Journal, Vol. 49, No. 2 (2011), pp. 324-339.

[13] J. Theis and H. Pfifer and P. J. Seiler, *Robust Control Design for Active Flutter Suppression*, AIAA Atmospheric Flight Mechanics Conference, AIAA SciTech Forum, (AIAA 2016-1751).

[14] F. Svoboda, *Damping system of aeroelasticity phenomena*, Master's thesis (2016), Czech technical university in Praque.

[15] R. L. Bispinghoff, H. Ashley, R. L. Halfman, *Aeroelasticity*, Dover publications, INC., 1996.

[16] M. R. Waszak, *Modeling Technology Active the Benchmark Design Active Model Applications Control for Control*, NASA Center for AeroSpace Information, June 1998.

[17] S. Afkhami and H. Alighanbari, *Nonlinear control design of an airfoil with active flutter suppression in the presence of disturbance*, IET Control Theory, Vol. 1, pp. 1638–1649.

[18] W. L. Keum and N. S. Sahjendra, *Adaptive Control of Multi-Input Aeroelastic System with Constrained Inputs*, Journal of Guidance, Control, and Dynamics, Vol. 38, pp. 2337–2350.

[19] J. M. Barker and G. J. Balas, *Comparing Linear Parameter-Varying Gain-Scheduled Control Techniques for Active Flutter Suppression*, Journal of Guidance, Control, and Dynamics, Vol. 23, pp. 948–955.

[20] J. S. Vipperman and J. M. Barker and R. L. Clark and G. J. Balas, *Comparison oc my and H_2 Synthesis Controllers on an Experimental Typical Section*, Journal of Guidance, Control, and Dynamics, Vol. 22, pp. 278–285.

[21] F. Svoboda, M. Hromčík, *Fixed-order H_∞ controllers for the Benchmark Active Control Technology (BACT) wing*, IFAC 2017 World Congress, Toulouse, France.